

Guideline for Yield Assessment in SHIP Plants

Uncertainties derived from the simulation approaches

IEA SHC TASK 64 | IEA SolarPACES Task IV | Solar Process Heat

Guideline for Yield Assessment in SHIP Plants: Uncertainties derived from the simulation approaches

**This is a report from SHC Task 64 /
SolarPACES Task IV: Solar Process Heat
and work performed in
Subtask C: Simulation and Design Tools**

Authors: José Miguel Cardemil, Alan Pino, Allan Starke, Ignacio Calderón-Vásquez, Ian Wolde, Carlos Felbol, Leonardo F.L Lemos, Vinicius Bonini, Ignacio Arias, Cristóbal Sarmiento, Javier Iñigo-Labairu, Jürgen Dersch

Date: October 16, 2023

DOI: 10.18777/ieashc-task64-2023-0001

The contents of this report do not necessarily reflect the viewpoints or policies of the International Energy Agency (IEA) or its member countries, the IEA Solar Heating and Cooling Technology Collaboration Programme (SHC TCP) members or the participating researchers.

Solar Heating and Cooling Technology Collaboration Programme (IEA SHC)

The Solar Heating and Cooling Technology Collaboration Programme was founded in 1977 as one of the first multilateral technology initiatives (“Implementing Agreements”) of the International Energy Agency.

Our mission is “*To bring the latest solar heating and cooling research and information to the forefront of the global energy transition.*”

IEA SHC members carry out cooperative research, development, demonstrations, and exchanges of information through Tasks (projects) on solar heating and cooling components and systems and their application to advance the deployment and research and development activities in the field of solar heating and cooling.

Our focus areas, with the associated Tasks in parenthesis, include:

- Solar Space Heating and Water Heating (Tasks 14, 19, 26, 44, 54, 69)
- Solar Cooling (Tasks 25, 38, 48, 53, 65)
- Solar Heat for Industrial and Agricultural Processes (Tasks 29, 33, 49, 62, 64)
- Solar District Heating (Tasks 7, 45, 55, 68)
- Solar Buildings/Architecture/Urban Planning (Tasks 8, 11, 12, 13, 20, 22, 23, 28, 37, 40, 41, 47, 51, 52, 56, 59, 63, 66)
- Solar Thermal & PV (Tasks 16, 35, 60)
- Daylighting/Lighting (Tasks 21, 31, 50, 61, 70)
- Materials/Components for Solar Heating and Cooling (Tasks 2, 3, 6, 10, 18, 27, 39)
- Standards, Certification, Test Methods and LCA/LCoH (Tasks 14, 24, 34, 43, 57, 71)
- Resource Assessment (Tasks 1, 4, 5, 9, 17, 36, 46)
- Storage of Solar Heat (Tasks 7, 32, 42, 58, 67)

In addition to our Task work, other activities of the IEA SHC include our:

- SHC Solar Academy
- *Solar Heat Worldwide*, annual statistics report
- SHC International Conference

Our members

Australia	European Copper Institute	SICREEE
Austria	France	Slovakia
Belgium	Germany	South Africa
Canada	International Solar Energy Society	Spain
CCREEE	Italy	Sweden
China	Netherlands	Switzerland
Denmark	Norway	Türkiye
EACREEE	Portugal	United Kingdom
ECREEE	RCREEE	
European Commission	SACREEE	

For more information on the IEA SHC work, including many free publications, please visit www.iea-shc.org.

Solar Power and Chemical Energy Systems Technology Collaboration Programme (IEA SolarPACES)

The SolarPACES Technology Collaboration Programme was founded in 1977 as one of the first multilateral technology initiatives ("Implementing Agreements") of the International Energy Agency.

Our mission is to facilitate technology development, market deployment and energy partnerships for sustainable, reliable, efficient and cost-competitive concentrating solar power technologies by providing leadership as the international network of independent experts.

To realize this mission, SolarPACES coordinates and advances concentrating solar technology research, by focusing on the next generation of technologies, by providing information and recommendations to policy makers and by organizing international conferences, workshops, reports and task meetings.

Our focus areas are organized in six tasks:

- Task I: Solar Thermal Electric Systems
- Task II: Solar Chemistry Research
- Task III: Solar Technology and Advanced Applications
- Task IV: Solar Heat Integration in Industrial Processes
- Task V: Solar Resource for High Penetration and Large-Scale Applications
- Task VI: Solar Energy and Water Processes and Applications

In addition to our Task work, other activities of the IEA SolarPACES include:

- SolarPACES International Conference.
- Review of CSP market and cost data with the International Renewable Energy Agency (IRENA).
- Joint project on solar resource for high penetration and large-scale applications in collaboration with the TCP on Photovoltaic Power Systems (PVPS TCP).
- Project in solar process heat in collaboration with the TCP on Solar Heating and Cooling (SHC TCP).

Our members

Australia	Austria	Brazil
Chile	China	European Commission
France	Germany	Greece
Israel	Italy	Mexico
Morocco	Namibia	Republic of Korea
South Africa	Spain	Switzerland
United Arab Emirates	United States of America	

For more information on the IEA SolarPACES work, including many free publications, please visit: www.solarpaces.org.

Contents

- Contents..... iv**
- 1 Introduction 1**
 - 1.1 Subtask C: Simulation and Design Tools 1
- 2 Methodology 2**
 - 2.1 Simulation Tools 3
 - 2.2 Case Studies 3
 - 2.2.1 Case A: Flat plate collectors 3
 - 2.2.2 Case B: Flat plate collectors with 1 axis tracking 4
 - 2.2.3 Case C: Linear Fresnel collectors 4
 - 2.2.4 Case D: Parabolic trough collectors 5
- 3 Uncertainty assessment 6**
- 4 Results 7**
 - 4.1 Case A: 7
 - 4.2 Case B: 8
 - 4.3 Case C: 8
 - 4.4 Case D: 9
- 5 Impact of common assumptions in SHIP simulations 10**
- 6 Induced error assessment in SHIP simulations 12**
 - 6.1 Case A 12
 - 6.2 Case B: 15
 - 6.3 Case C: 18
 - 6.4 Case D: 20
- 7 Conclusions and outlook 22**
- 8 References 23**
- 9 Appendix: Simulation Tools for Solar Thermal Systems 24**



1 Introduction

Solar thermal technologies have been recognized as a reliable option for delivering process heat to industrial processes (Farjana et al. 2018; Sharma et al. 2017), and have been a subject of study in two previous Tasks of the Solar Heating and Cooling Program (SHC), Task 33 and Task 49, and it represents a permanent task in Solar-PACES: Task IV. Despite the efforts and progress achieved to build new knowledge and reduce the entry barriers that solar thermal technologies face in the heat market for industry, the number of solar heat plants coupled with industrial processes is less than 1,000 installations (Weiss and Spörk-Dür 2020). In that context, since 2020, Task 64/IV has started a collaborative effort bringing together the experience from professionals, project developers, and scientists, aiming to address part of the entry barriers that hinder the further development of the market.

The questions addressed in the context of the Task are the standardization of integration schemes at the process and supply levels, as well as the combination with other efficient heat supply technologies such as combined heat and power plants, heat pumps, or power-to-heat. In addition, the identification of standardized industrial load profiles and the uncertainties associated with the simulation tools commonly used for yield assessment. In that context, Task 64/IV organized its work into five subtasks.

1.1 Subtask C: Simulation and Design Tools

Subtask C aims to address the issue that, within the SHIP¹ industry, several simulation tools are available, and the results delivered by each tool may differ significantly from each other. Therefore, Task 64 / IV Subtask C aims to integrate the knowledge base established in the previous Tasks 33 and 49, taking the information according to the industry's "common language", bringing together the knowledge and experience of several experts working with heat integration and heat management tools. In that context, the main objective of the subtask is to develop a deep analysis of the available simulation and monitoring tools for assessing the potential benefits of integrating solar heat into industrial processes, with known uncertainty sources. To achieve the objective, a series of activities are carried out, comprising the identification of the simulation tools currently available, the classification of such tools according to their capabilities, simulation approaches, and software restrictions. In addition to that, four case studies have been defined, which allow us to conduct equivalent simulations in different tools, and compare the results, identifying the differences and the impact on the main performance indicators. Thus, this document summarizes the results of that analysis, which constitutes a guide for the development of the yield assessment of SHIP plants.

¹ SHIP: Solar Heat for Industrial Processes

2 Methodology

For the specific activities that are covered in this study, that is, the assessment of deviations in simulation tools, the highlighted section of the flowchart presented in **Error! Reference source not found.** has been followed. First, a case study is selected. This means specifying a solar thermal installation currently in operation or being built, from which enough detailed information regarding the design (either public or private) it is available and can be used to model the system in a simulation tool for energy yield assessment. For instance, the information should include the model of the collector employed (or performance curve), size, orientation, and slope of the solar field, size, geometry, and insulation characteristics of the thermal storage (if available), details of heat exchangers, load profile (mass flow and temperature), and finally the control philosophy (including pump features).

In a second stage, when all the technical information has been defined, it is compiled in a unique file (spreadsheet format) that is distributed to the simulation specialists, who develop their simulation in their own simulation tool or commercial tool in which they are trained. In addition to the technical features, the meteorological information (TMY format) is provided along with a template spreadsheet to report the simulation results.

Once the results from the different analysts have been received, they are compared according to the metrics selected for this purpose, as detailed in Section 2.2. The comparisons are made considering different control volumes of the plant, according to the stages of energy flow, i.e., in the solar field, in thermal storage, and in the load to process. To assess the differences in the results reported, four timescales are considered for the comparison routine: hourly, daily, monthly, and annual values.

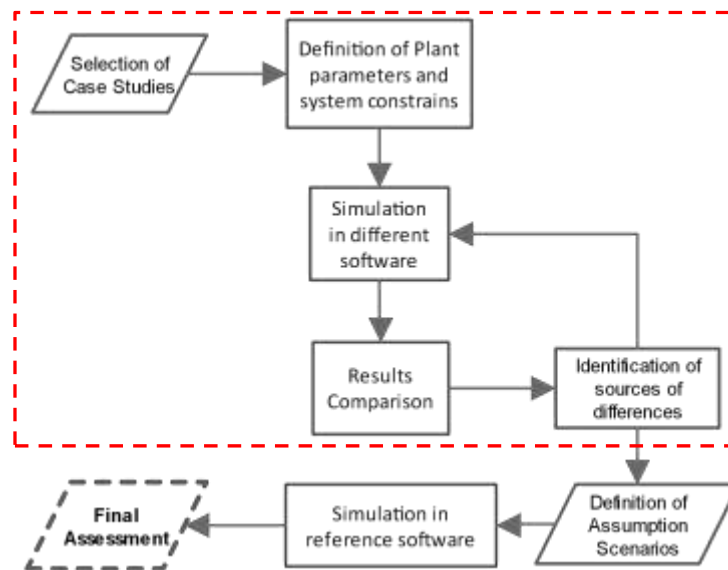


Figure 1: Flowchart of the methodology utilized to identify the sources of differences in the energy yield results performed by different analysts employing different simulation tools (software).

As a result of the comparison, the main sources of deviations between the results of each simulation tool and the results of the reference tool are identified and quantified in a preliminary manner, according to the metrics used. To improve qualitative analysis, bilateral meetings were held between the core team and each of the analysts during the first semester of 2021. The objective of these meetings is to understand the reasoning behind the assumptions that the analysts have considered, differentiating when they are due to lack of information about the system design, from the intrinsic limitations of modeling approach and resolution strategy of the specific software employed.

Feedback to the analysts is also given, based on the comparison of results. The aim is to enhance their models by improving the assumptions made due to lack of information, but not to alter the results to be closer to the reference tool results. Hence, a second round of simulation is carried out, allowing to compare the results, and conduct equivalent analysis that leads the identification of sources of differences.

The final steps of the assessment performed, which are not presented in this study, include the last three stages of the flow chart in Fig. 1. The sources of differences are categorized according to the impact on the final energy yield. Since different software and different analysts might increase the bias and uncertainties in the analysis, a parametric analysis is performed by varying the parameters associated with the sources of differences previously identified.

This parametric analysis is carried out using one single reference tool and by the same analyst with the aim of isolating (or reducing) the impact of the human factor. Finally, the final impact assessment and sources of differences are established.

2.1 Simulation Tools

There was no restriction criterion for selecting the simulation tools. Any participant in Subtask C who was trained in a simulation tool and willing to contribute was welcome. Therefore, it was possible to include licensed software, open source software, and companies internal software in the study. The participants/analyst also delivered a brief simulation log together with the results where the main assumptions and limitations of the software for a specific component were indicate, e.g., if the software cannot model the thermal storage losses, a penalizing factor is added by the analyst to the energy yield. Table 1 summarizes the tools/software employed for each case study.

Table 1: List of tools/software employed for the different case studies (see app for more details).

Case study A	CEA model, Greenius, SHIP2FAIR tool, SHIPcal, System Advisor Model (SAM) TRNSYS - TESS library, TRNSYS - basic library.
Case study B	NewHeat tool, Polysun, SHIP2FAIR tool, TRNSYS (3 simulations using different libraries)
Case study C	Greenius, SAM, Scilab, SHIP2FAIR tool, SHIPcal, TRNSYS (4 simulations using different libraries)
Case study D	Greenius, Polysun, TRNSYS, SHIP2FAIR tool

2.2 Case Studies

The information presented in this section summarizes the main plant parameters and the operation scheme for each case study. However, more information is available and is supplied to the analyst to build the simulation models, especially regarding hourly load profile, efficiency of solar field, geometry and insulation of the storage, effectiveness of the HXs, pump mass flow and efficiency, control philosophy, among others.

2.2.1 Case A: Flat plate collectors

The system supplies heat to a copper electrowinning plant located in the Atacama Desert, Chile (lat. 23.45° S, long. 68.81° W, annual GHI 2,631 kWh/m²). The plant is made up of a 39,300 m² solar field of fixed flat plate collectors, with a thermal storage tank of 4,300 m³. The coupling scheme is considered through two heat exchangers, one between the solar field and the thermal storage tank, and the other between the storage and the load. A simplified layout for the plant is depicted in **Error! Reference source not found.**. The heat transfer fluid (HTF) considered in the solar field is a water-glycol mixture (33% glycol), while the energy storage system uses demineralized water. Furthermore, the heat transfer fluid of the process is water, where the set point temperature of the process is 70 °C and the return temperature is 40 °C. The annual heat demand is 94,171 MWh with a constant load profile (24/7) (Quiñones et al. 2020).

The solar field circuit is controlled by a differential temperature controller, which activates the circulation pump when the solar field outlet temperature is higher than the temperature at the bottom of the storage tank plus a dead band of 10 °C. Furthermore, it is considered that a lower dead band of 2 °C turns off the pump. The temperature at the top of the tank is monitored for safety purposes to avoid boiling, so it deactivates the pump when it reaches 100 °C. On the thermal storage side and the load circuit, since there is a fixed mass flow pump, the HX that supplies the load has a bypass to avoid heating the water to the process over 82.6 °C.

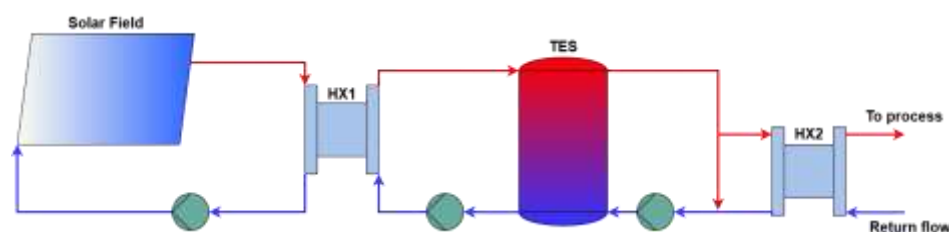


Fig. 1. System diagram of case study A, flat plate collectors to supply hot water to a copper mining process.

2.2.2 Case B: Flat plate collectors with 1 axis tracking

In Case B, the system supplies hot water as a preheating stage of a gas boiler coupled to a paper mill factory located in Dordogne, France. The total gross collector area is 4,212 m², and the storage tank volume is 457 m³. The solar collectors are installed on a 1-axis tracking system that allows to increase the energy absorbed by the solar field, and consequently, the heat production. The heat output can also be reduced by increasing the solar incident angle on purpose if necessary. The primary circuit (solar field) employs a water-glycol mixture as heat transfer fluid (HTF). The make-up water to be heated is continuously provided by the demineralized unit of the paper mill. Both the primary and secondary circuits employ variable-speed pumps controlled to maximize solar field output. The layout is depicted in Fig. 2. There is no fixed set-point temperature for the water delivered by the solar plant to the process. The temperature set-point to be reached at the collector outlet evolves throughout the year from 30 °C (in winter) to 90 °C (in summer), in order to maximize the production of solar heat. This allows to increase the total annual heat supplied. However, the maximum temperature of the feedwater for the boiler is 80 °C.

The control strategy is the following. (a) when a threshold of irradiance on the surface of the collector is reached, the pump on the solar field circuit is turned on. At this point there is recirculation only on the solar field until the set temperature at the solar field outlet is reached (variable throughout the year). (b) When the set temperature is achieved at the solar field circuit, the flow passes through the heat exchanger (HX), and the pump of the secondary circuit is turned on. The pump operates in a closed circuit between the HX1 and thermal storage. (c) When the process demands heat, water from the top of the thermal storage is employed. At the same time, cold water is pumped into the bottom of the tank to keep the volume constant.

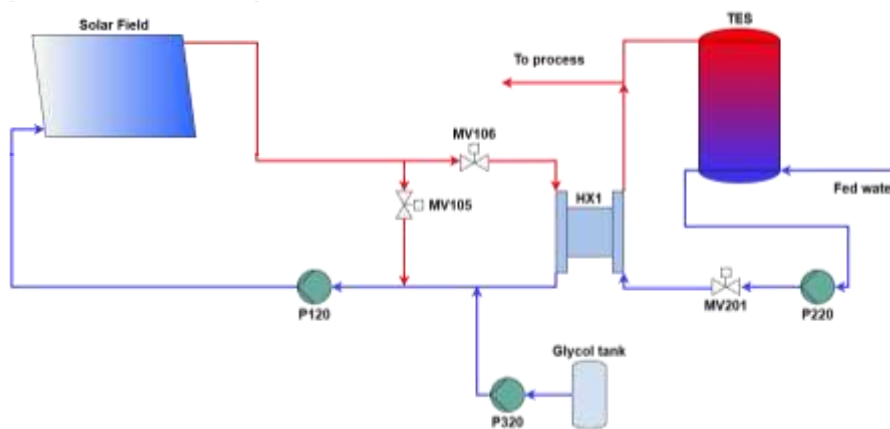


Fig. 2. System diagram of case study B, 1-axis tracking flat plate collectors to supply hot water to a paper mill process.

2.2.3 Case C: Linear Fresnel collectors

The system analyzed in Case C corresponds to a system configured by the company Solatom, which consists of Fresnel FTL20 solar collectors. FLT20 modules are pre-assembled and packed at the factory, and then transported ready to be installed. The module has an aperture area of 26.4 m², that allows delivering a thermal power of 14.5 kW_{th}, when operating at 1000 W/m² of DNI. In addition, such collector is suitable for installation on rooftops. The system operates in the direct steam generation (DSG) scheme and is located in Seville (Spain), integrated in recirculation mode with a steam drum. The water-steam mixture generated by the solar field feeds the steam-drum, where the saturated liquid is fed back to the collector loop by the circulation loop. In case of sufficient pressure in the steam drum, the saturated steam is fed into the conventional steam circuit (load). The total area of the reflective surface is 1900.8 m² and is structured in 6 loops with 12 modules each (the area of a single module is 26.4 m²). The layout of the plant is depicted in Fig. 3. The annual heat demand is 4,858 MWh and the typical load curve for a day is presented in (de Santos López 2021). Saturated steam is provided at 6 bar (158.5 °C) to the process, with the condensates returning at 70 °C. The demand for steam should be provided by the solar system with the aid of a conventional natural gas boiler installed in parallel with the solar field (not considered in the simulations), to ensure the demand is met during periods of low irradiation.

The control system is configured to maintain the operation conditions of the plant following these settings: (a) start-up: boiler feed water recirculates in the field steam drum loop until pressure reaches the requirements; (b) normal

operation: the steam from the steam drum is delivered to the steam line; (c) shutdown: decreases the mass flow rate as irradiation decreases, reaching a minimal value, considering the following logic: if the nominal conditions could be met, go to recirculation; if the minimal flow rate is larger than the demand, go to recirculation; for operation on nighttime and/or low solar resource: "minimum flow rate in single collector loop".

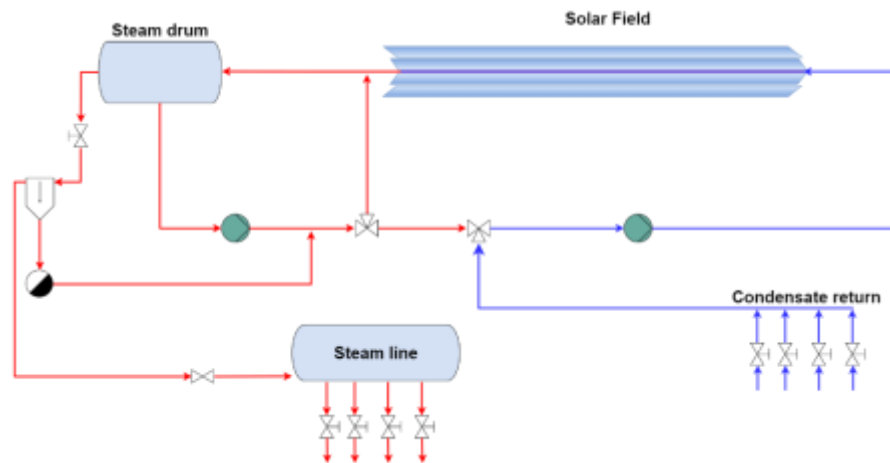


Fig. 3. System diagram of case study C, linear Fresnel collector (LFR) for direct steam generation.

2.2.4 Case D: Parabolic trough collectors

The system considered for Case D consists of a PTC collector field installed on the roof of a dairy factory and is based on an existing system located in Saignelégier, Switzerland. A total of 17 PTC collector rows are installed, where one collector per row is implemented. The solar field operates with a water-glycol mixture, which is heated to a design temperature of 110 °C. The HTF is sent to a heat exchanger with a nominal heat transfer rate of 350 kW. The thermal energy from the collectors is used to heat the pressurized water of the process up to a design temperature of 105 °C. This heated water flows to the boiler and storage system of the plant, from where it is distributed to the processes involved in dairy production. A simplified layout of the plant is depicted in Fig. 4.

The control strategy considered for the system is the following. When heat is required, and the direct solar radiation exceeds a predefined threshold (250 W/m²), the collectors are automatically turned towards the Sun and the pump starts to circulate. The flow rate in the solar circuit is controlled by a frequency converter to maintain the set temperature (between 110 and 120 °C). If this temperature exceeds the maximum allowed value, the sensor defocuses automatically. High-temperature shut-off occurs only if high flow is detected. A shut down occurs when the direct solar irradiance is lower than 100 W/m².

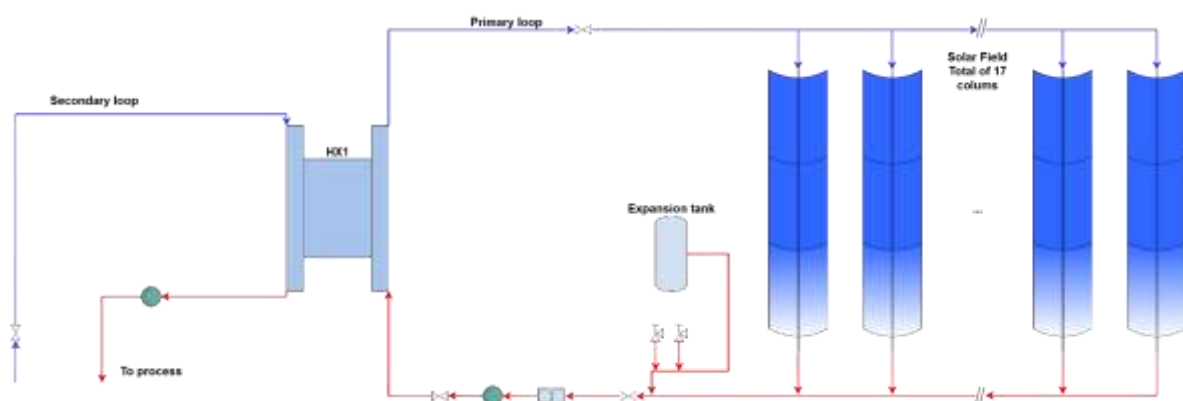


Fig. 4. System diagram of case study D, parabolic trough collectors to supply hot water to a dairy process.

3 Uncertainty assessment

In order to configure a flexible tool for comparing the different simulation results of the cases under study, a unified open-source script for the treatment of hourly, daily, monthly, and annual time series has been programmed using Python. For each case study, one of the available simulation results was selected to be employed as reference for the corresponding results comparison. Therefore, the normalized root mean square (nRMSE), the normalized mean bias error (nMBE), the relative difference, the root mean square difference of the pattern (RMSD), Pearson correlation coefficient (R), and the standard deviation (σ) were calculated as established statistical comparison metrics. The pattern root mean square difference is presented in eq. 1.

$$RMSD = \sqrt{B + \sigma_{ref}^2 + \sigma_{est}^2 - 2\sigma_{est}\sigma_{ref}R} \quad (\text{eq. 1})$$

where σ_{est} and σ_{ref} are the standard deviation of the scenario analyzed and the reference, R is the Pearson correlation between the scenario analysed and reference, and B represents the bias between the data sets.

Furthermore, the Dynamic Time Warping (DTW) algorithm was used for analyzing hourly results as a method to size and compare the time series difference between the results reported by the reference and other tools, with respect to certain parameters. Currently, DTW is used in similarity tests, also for clustering and machine learning algorithms (Zhang et al. 2021). The purpose of using the DTW in this study is to quantify phase and amplitude errors, as well as to contrast the similarity between the temporal sequences with respect to the reference, and the sensitivity and relationship of the DTW with other statistical established metrics (Gaspar et al. 2017). The main advantage of DTW over other established statistical metrics, such as RMSE and MBE, is related to the reliable alignment between the reference and test patterns. However, one of the main disadvantages of using DTW is related to a more robust computational effort to find the optimal alignment path in time (Brown and Rabiner, 2005).

Although the RMSE is more intuitive, it reports on the average size of the for those errors regardless of their sign (over or underestimation). Therefore, the greatest advantage of the RMSE is related to the measurement of uncertainty in the calculation of forecasts. However, two important disadvantages are observed, related to the fact that it is an absolute uncertainty metric that makes a comparison through highly variable time series and that it is influenced by outliers. Therefore, it is not used to see the dynamic evolution of the series (Li et al. 2020; Gaspar et al. 2017; Brown and Rabiner 2005) .

Although the DTW is useful to determine the impacts that each assumption may cause in the alignment of two time series, it is crucial to determine in the hourly scale whether the simulation is above or below the reference value, i.e., underestimating or overestimating the yield of the SHIP system. Thus, the residual values are calculated by means of the instantaneous difference between the reference and the induced error scenario. A thorough analysis through this methodology is described in (Cardemil et al. 2022)

4 Results

The main results of the study assess the “deviations” observed between the simulation results of the reference set of results and those shared by the different analysts. These “deviations” are quantified employing the metrics described in Section 2.2. The reference tool is named tool 0 for all case studies, and corresponds, when available, to the tool employed by the project developer during the design stage of the SHIP plant. The tools have been randomly numbered for the benchmark analysis to avoid the unintended message of ranking the tools.

4.1 Case A:

The annual and monthly energy delivered to the load by the plant considered in Case A are presented in Fig. 5. It can be observed that in the annual analysis tools 1 and 2 overestimate the energy yield, and tools 3, 4, 5, and 6 underestimate it. There are no large differences between the values in the tools (up to 6.45 %), with the exception of tool 5 which underestimates the energy to the load by 20.3 % compared to the reference. The monthly results indicate a similar behavior in the shape of curves, but certain values strongly disagree. For example, tool 5 delivers 35 % less energy to the load compared to the reference in June.

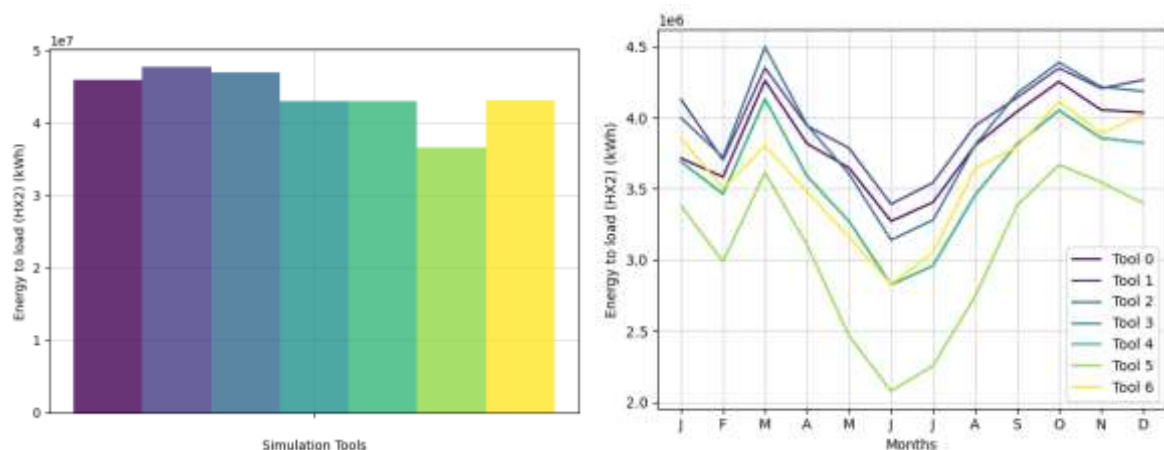


Fig. 5. Annual and monthly figures of energy yield to load obtained by the different tools for case A.

Fig. 6 presents a daily comparison of the different DTW profiles between the reference tool and the other tools used in the analysis (plots on the left side). The comparison is shown in terms of the solar radiation absorbed solar radiation (q_{in}), heat to the TES² (q_{hx1}), and the heat to the load (q_{hx2}). The first plot shows a low value for the DTW for all tools, with the exception of Tool 6 (yellow lines), suggesting that a different approach to dealing with the meteorological input was used for this simulation. This situation persists in the other comparisons. For the rest of the tools, it is noticeable that the indicator increases its value as it goes through the control volumes in the direction of the energy flow (from irradiation to load). Therefore, it is observed that the different assumptions and simulation approaches may contribute to the overall error as the simulation increases its components. On the plots on the right side of Fig. 6, certain days are selected to present the hourly evolution. It can also be observed that tool 6 has a mismatch in the radiation data compared to the rest. In addition, for the heat supplied to the load (q_{hx2}), it is observed how the thermal storage is modeled. The periods where the curve saturates to a constant value are explained by assuming a modelling approach considering a single node tank. Thus, it charges and discharges at continuous energy rates between the set temperature and the minimum temperature. On the other hand, periods where the curve increases and decreases with a steady slope means that the tank is stratified. Hence, the tank can deliver lower energy rates due to a lower outlet temperature.

² TES: Thermal Energy Storage

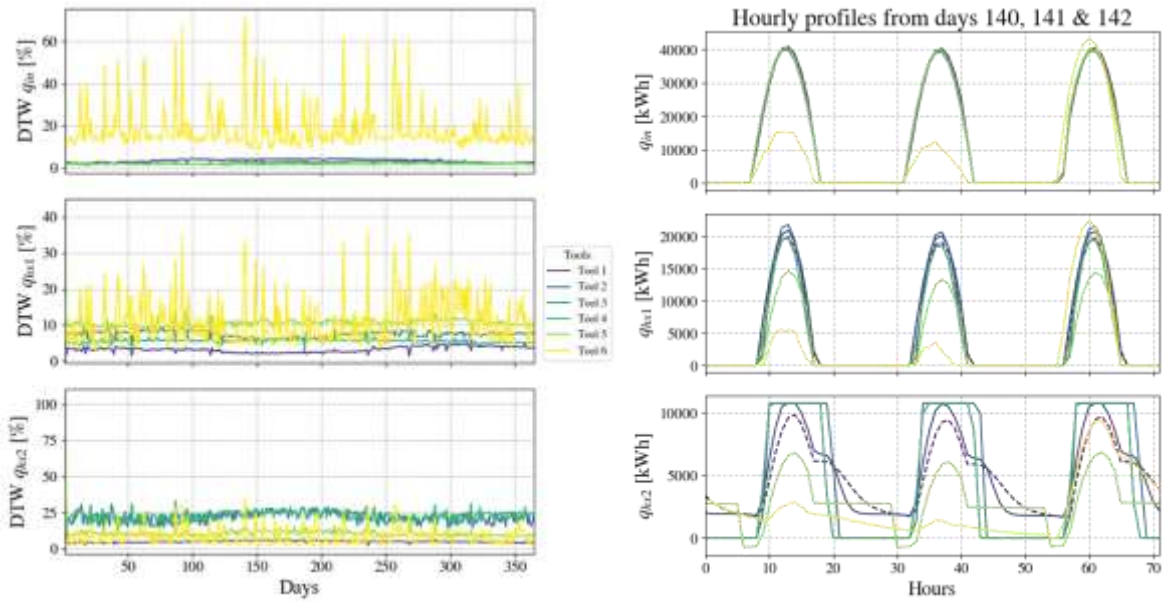


Fig. 6. Dynamic Time Warping (DTW) on the daily timescale (left) and hourly profiles for selected days (right) for Case A.

4.2 Case B:

Annual and monthly values of energy yield to the load for case B are presented in Fig. 8. In this case, results reported by Tools 1 and 4 are similar to the reference tool in both annual and monthly time resolution, revealing an annual difference under 1 %. On the other hand, results reported by Tools 2, 3 and 5 underestimate annual and monthly values of energy delivered to the load. This difference is -8.3 % for tool 3, -27 % for tool 5 and -49 % for tool 2 for annual figures. The monthly results are consistent with the annual values. However, there is a trend during certain months of the year, where the difference between some tools and the reference tool is higher, i.e., Tools 2, 3, and 5. This difference increases during the summer months with higher solar resource availability. Conversely, during the winter months, such as December or January, there are smaller absolute differences compared to the reference tool.

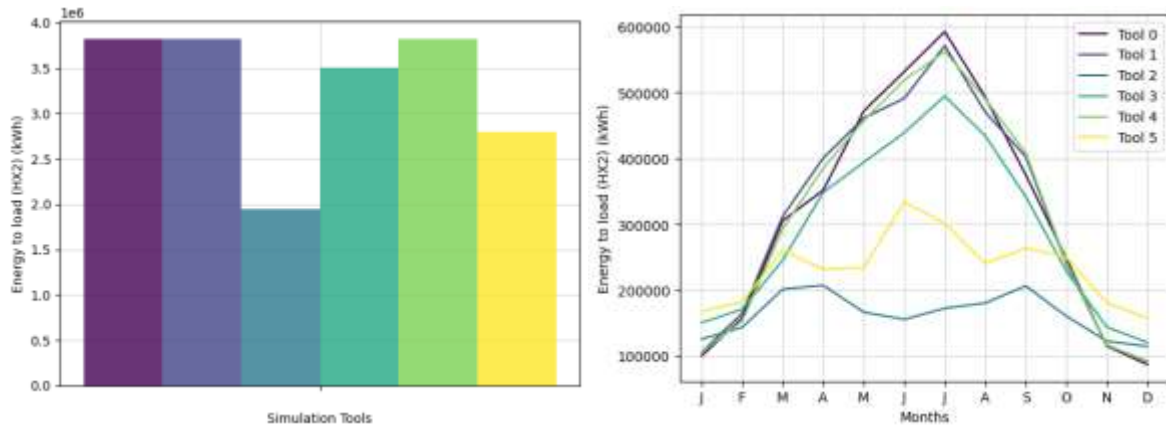


Fig. 7. Annual and monthly figures of the energy yield to the load obtained by the different tools for case B.

4.3 Case C:

The annual and monthly values of the energy yield to the load for case C are presented in Fig. 9. In this case, the results reported by tools 1, 3, 5, 6, and 7 are similar to the reference tool, with an annual deviation below 10 %. Furthermore, the results reported by tools 4 and 8 underestimate the annual energy delivered to the load, with an overall difference of -19.5 % and -17.7 %, respectively. For monthly results, Tool 8 mainly underestimates in summer (April to September). Moreover, Tool 4 is close to the reference in July and August, it consistently

underestimates the energy yield from November to June, and overestimates in September and October. On the other hand, Tool 2 presents the largest difference with the reference tool. It presents significantly higher values, for both annual and monthly results, overestimating in 84.2 % the reference annual value.

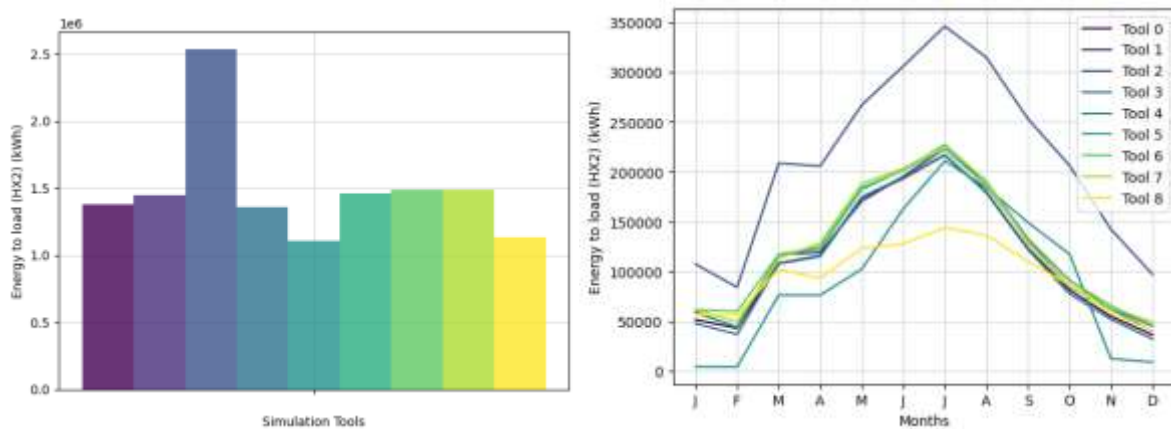


Fig. 8. Annual and monthly figures of energy yield to load obtained by the different tools for case C.

4.4 Case D:

For case study D, only 3 sets of results have been collected. Therefore, the comparison analysis has not been concluded. However, Fig. 8 presents the annual and monthly results. As preliminary observations, for annual values, tool 1 underestimates (-11 %) and tool 2 greatly overestimates the energy supplied to the load (41.9 %). When the monthly figures are observed, it is noticeable that Tool 1 underestimates the energy yield in the winter months but overestimates it in summer. Tool 2 has a strange behavior with high peaks in March and June, which leads to an overestimate of the overall energy yield.

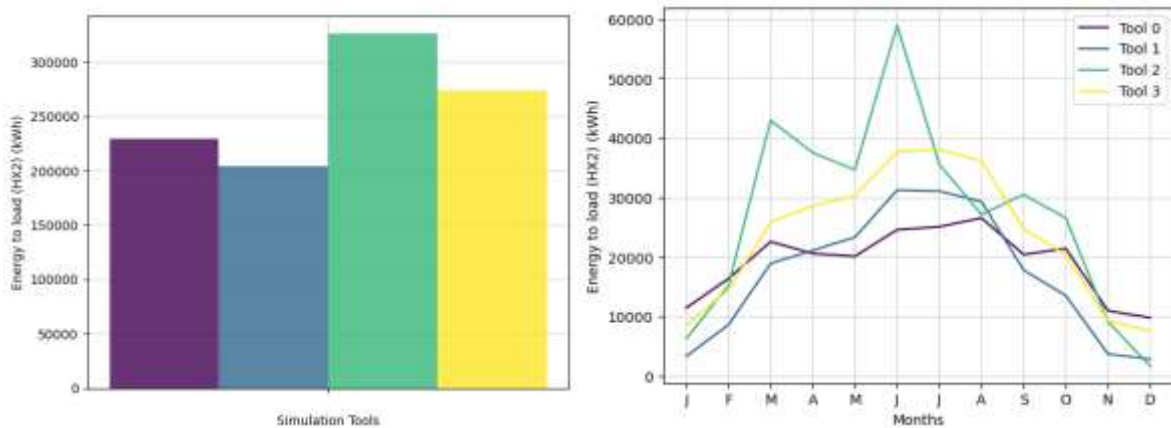


Fig. 9. Annual and monthly figures of the energy yield to the load obtained by the different tools for case D.

5 Impact of common assumptions in SHIP simulations

To summarize the results from the comparison analysis, Tab. 3 present the differences observed in the total energy yield to the load in monthly and annual values for the 4 case studies. The normalized RMSE is presented for the monthly values and the percentual difference is presented for the annual values, when compared to the reference tool of each case study.

Tab. 2. Summary of the differences observed from the simulations in the four case studies.

Case	Value	Time scale	Metric	Tool 1	Tool 2	Tool 3	Tool 4	Tool 5	Tool 6	Tool 7	Tool 8
A	Energy to load	Monthly	nRMSE	0.05	0.04	0.07	0.07	0.21	0.08	-	-
		Annual	% diff.	4.03	2.32	-6.5	-6.5	-20.3	-6	-	-
B	Energy to load	Monthly	nRMSE	0.07	0.69	0.18	0.06	0.49	-	-	-
		Annual	% diff.	-0.05	-49	-8.3	-0.12	-26.8	-	-	-
C	Energy to load	Monthly	nRMSE	0.06	0.88	0.02	0.33	0.07	0.09	0.08	0.31
		Annual	% diff.	5.30	84.2	-1.6	-19.5	6.1	8.3	8	-17.7
D	Energy to load	Monthly	nRMSE	0.31	0.74	-	-	-	-	-	-
		Annual	% diff.	-11	41.9	-	-	-	-	-	-

In addition, Tab. 4 presents the values for the DTW in the hourly comparison, normalized by the annual load. The table is separated by case study and tools, and for each case study different control volumes are analyzed, i.e. the supplied energy is calculated at different stages of the energy flow to the load. For example, for case study A three control volumes are considered: (a) solar field, where the incident radiation on the collector's surface is calculated, (b) heat exchanger between solar field and storage tank, where the energy transferred to the tank is calculated, and finally (c) heat exchanger between the storage tank and the load, where the total energy yield to the load is calculated. The DTW represents a cumulative distance from the reference, hence lower DTW are desirable. It can be observed that DTW increases (maximum values) when the control volume is closer to the load. It means that the deviations of the simulation results at different components impact the next component on the direction of the energy flow to the load. Sometimes, the monthly and annual values hide certain differences when integrating the values over the period, as positive and negative deviations are compensated.

From the analysis of the DTW results and the direct comparison of the hourly curves, the main sources of difference are identified. For example, time delays or shifting between reference and tools are due to a shift in the sun position, consideration or not of the heat capacitance of the components and modeling of the control philosophy. In addition, certain absolute differences of energy flow are due to modeling of the thermal storage (stratified, hot, and cold tanks, or fully mixed), modeling of the heat exchangers, and considering the thermal losses of piping.

Tab. 3. Summary of the comparison results in terms of the DTW

Case	Parameter	Normalized DTW %	Tool 1	Tool 2	Tool 3	Tool 4	Tool 5	Tool 6	Tool 7	Tool 8
A	Incident radiation	min	1.34	1.07	1.45	1.45	1.12	8.73	-	-
		max	4.41	4.42	3.61	3.61	2.79	71.83	-	-
	Energy to TES	min	1.44	3.69	3.63	3.63	7.73	3.38	-	-
		max	9.25	9.24	8.84	8.84	42.79	32.34	-	-
	Energy to load	min	2.51	13.12	11.54	11.54	7.44	1.83	-	-
		max	56.03	32.99	31.83	31.83	104.91	35.78	-	-
B	Incident radiation	min	0.30	0.53	0.29	0.24	0.29	-	-	-
		max	7.61	33.82	11.21	10.59	26.95	-	-	-
	Energy to TES	min	0.00	0.07	0	0	4.21 e-05	-	-	-
		max	9.91	37.46	13.46	17.21	20.39	-	-	-
	Energy to load	min	0.04	0.07	0.79	0.38	0.57	-	-	-
		max	21.0	65.47	38.64	20.24	34.76	-	-	-
C	Incident radiation	min	8.02 e-8	5.33 e-17	~ 0	~ 0	0.29	NA	0	0
		max	0.014	5.39	0.004	2.13	16.39	NA	1.45 e-14	1.45e-14
	Energy to load	min	0	0.42	0	0.23	3.10 e-05	NA	0	0
		max	5.56	34.98	19.72	18.67	18.78	NA	15.06	18.99
D	Incident radiation	min	2.21	3.15	-	-	-	-	-	-
		max	14.27	85.93	-	-	-	-	-	-
	Energy to load	min	0.19	0.19	-	-	-	-	-	-
		max	47.46	138.65	-	-	-	-	-	-

Notes: - For case A, Tool 6 presents a high DTW value for the incident radiation due to a shift in the operation start time. - For case C, tool 6 did not report hourly results.

6 Induced error assessment in SHIP simulations

To gain a deeper understanding of the impact that different assumptions made during the modelling stage of components and software limitations have on the outcome of the simulation, a different approach was proposed. Here, several errors and assumptions are forced into the simulation model parameters for each case study's reference case to induce errors in the results, and hence quantify and relate the simulation input "deviation/error" with the "deviation" of the results. Consequently, several scenarios were created for each case study, where the input deviations are clearly stated. This assessment was performed for cases B, C, and D.

6.1 Case A

<i>Scenarios</i>	<i>Time Shifting [h]</i>	<i>Thermal Capacitance [%]</i>	<i>Thermal Insulation (cm)</i>	<i>HX Effectiveness [%]</i>	<i>TES nodes [-]</i>	<i>Load</i>
<i>Scenario 0</i>	0	5	5	70	20	Std
<i>Scenario 1</i>	1	5	5	70	20	Std
<i>Scenario 2</i>	0,5	5	5	70	20	Std
<i>Scenario 3</i>	-1	5	5	70	20	Std
<i>Scenario 4</i>	-0,5	5	5	70	20	Std
<i>Scenario 5</i>	0	0,0001	5	70	20	Std
<i>Scenario 6</i>	0	150	5	70	20	Std
<i>Scenario 7</i>	0	200	5	70	20	Std
<i>Scenario 8</i>	0	250	5	70	20	Std
<i>Scenario 9</i>	0	300	5	70	20	Std
<i>Scenario 10</i>	0	5	Underground	70	20	Std
<i>Scenario 11</i>	0	5	10	70	20	Std
<i>Scenario 12</i>	0	5	5000	70	20	Std
<i>Scenario 13</i>	0	5	5	60	20	Std
<i>Scenario 14</i>	0	5	5	80	20	Std
<i>Scenario 15</i>	0	5	5	100	20	Std
<i>Scenario 16</i>	0	5	5	70	10	Std
<i>Scenario 17</i>	0	5	5	70	2	Std
<i>Scenario 18</i>	0	5	5	70	1	Std
<i>Scenario 19</i>	0	5	5	70	20	0-0
<i>Scenario 20</i>	0	5	5	70	20	2-2

Case A

<i>Control Volume</i>	<i>Energy to load</i>	
<i>Parametric analysis</i>	<i>nRMSE</i>	<i>%DIF</i>
<i>Scenario 1</i>	0,17	-6,46
<i>Scenario 2</i>	0,09	-1,34
<i>Scenario 3</i>	0,16	-5,33
<i>Scenario 4</i>	0,09	-0,95
<i>Scenario 5</i>	0,03	0,78
<i>Scenario 6</i>	0,02	-0,72
<i>Scenario 7</i>	0,04	-1,53
<i>Scenario 8</i>	0,05	-2,37
<i>Scenario 9</i>	0,07	-3,26
<i>Scenario 10</i>	0,00	-0,02
<i>Scenario 11</i>	0,00	0,16
<i>Scenario 12</i>	0,01	0,42
<i>Scenario 13</i>	0,09	-2,95
<i>Scenario 14</i>	0,08	2,19
<i>Scenario 15</i>	0,22	4,96
<i>Scenario 16</i>	0,10	-0,40
<i>Scenario 17</i>	0,34	-6,28
<i>Scenario 18</i>	0,42	-13,67
<i>Scenario 19</i>	0,07	-0,55
<i>Scenario 20</i>	0,23	-5,33

Case A

Control Volume	Energy to load		
Parametric analysis	Maximum normalized residual error	Minimum normalized residual error	Standar deviation
Scenario 1	0,377	-0,247	0,072
Scenario 2	0,232	-0,211	0,043
Scenario 3	0,276	-0,344	0,07
Scenario 4	0,162	0,223	0,041
Scenario 5	0,062	-0,074	0,013
Scenario 6	0,056	-0,017	0,008
Scenario 7	0,101	-0,03	0,015
Scenario 8	0,134	-0,044	0,022
Scenario 9	0,168	-0,056	0,03
Scenario 10	0	-0,001	0
Scenario 11	0,014	-0,009	0,001
Scenario 12	0,032	-0,013	0,002
Scenario 13	0,107	-0,049	0,039
Scenario 14	0,051	-0,102	0,037
Scenario 15	0,158	-0,265	0,097
Scenario 16	0,168	-0,069	0,047
Scenario 17	0,471	-0,146	0,152
Scenario 18	0,579	-0,129	0,18
Scenario 19	0,18	-0,139	0,031
Scenario 20	0,691	-0,344	0,104

6.2 Case B:

Scenarios	Time Shifting	Multiple for thermal cap.	Thermal Capacitance	Thermal Insulation	HX Effectiveness	Multiple for TES nodes	TES nodes	Tracking system
Scenario 0	0	1	10.2	5/4.3	91	1	50	-44 to +44
Scenario 1	1	1	10.2	5/4.3	91	1	50	-44 to +44
Scenario 2	0.5	1	10.2	5/4.3	91	1	50	-44 to +44
Scenario 3	-1	1	10.2	5/4.3	91	1	50	-44 to +44
Scenario 4	-0.5	1	10.2	5/4.3	91	1	50	-44 to +44
Scenario 5	0	0	0.0001	5/4.3	91	1	50	-44 to +44
Scenario 6	0	1.5	15.3	5/4.3	91	1	50	-44 to +44
Scenario 7	0	2	20.4	5/4.3	91	1	50	-44 to +44
Scenario 8	0	2.5	25.5	5/4.3	91	1	50	-44 to +44
Scenario 9	0	3	30.6	5/4.3	91	1	50	-44 to +44
Scenario 10	0	1	10.2	0/0	91	1	50	-44 to +44
Scenario 11	0	1	10.2	5000	91	1	50	-44 to +44
Scenario 12	0	1	10.2	5/4.3	60	1	50	-44 to +44
Scenario 13	0	1	10.2	5/4.3	80	1	50	-44 to +44
Scenario 14	0	1	10.2	5/4.3	100	1	50	-44 to +44
Scenario 15	0	1	10.2	5/4.3	91	0.5	25	-44 to +44
Scenario 16	0	1	10.2	5/4.3	91	0.1	5	-44 to +44
Scenario 17	0	1	10.2	5/4.3	91	fully-mixed	1	-44 to +44
Scenario 18	0	1	10.2	5/4.3	91	1	50	-90 to +90
Scenario 19	0	1	10.2	5/4.3	91	1	50	-30 to +30

Case B

Control Volume	Energy to load	
<i>Parametric analysis</i>	nRMSE	%DIF
<i>Scenario 1</i>	0,193	-5,056
<i>Scenario 2</i>	0,000	0,000
<i>Scenario 3</i>	0,000	0,000
<i>Scenario 4</i>	0,180	-4,011
<i>Scenario 5</i>	0,039	2,262
<i>Scenario 6</i>	0,025	-1,403
<i>Scenario 7</i>	0,051	-2,877
<i>Scenario 8</i>	0,087	-4,505
<i>Scenario 9</i>	0,126	-5,971
<i>Scenario 10</i>	0,012	-0,967
<i>Scenario 11</i>	0,009	0,705
<i>Scenario 12</i>	0,154	-6,009
<i>Scenario 13</i>	0,053	-1,668
<i>Scenario 14</i>	0,042	1,155
<i>Scenario 15</i>	0,116	0,509
<i>Scenario 16</i>	0,114	-0,787
<i>Scenario 17</i>	0,384	-9,697
<i>Scenario 18</i>	0,315	1,296
<i>Scenario 19</i>	0,297	-4,032

Case B

<i>Control Volume</i>	Energy to load		
<i>Parametric analysis</i>	Maximum normalized residual error	Minimum normalized residual error	Standar deviation
<i>Scenario 1</i>	0,411	-0,152	0,041
<i>Scenario 2</i>	0	0	0
<i>Scenario 3</i>	0	0	0
<i>Scenario 4</i>	0,229	-0,381	0,038
<i>Scenario 5</i>	0,034	-0,071	0,006
<i>Scenario 6</i>	0,069	-0,02	0,004
<i>Scenario 7</i>	0,125	-0,062	0,009
<i>Scenario 8</i>	0,251	-0,069	0,016
<i>Scenario 9</i>	0,329	-0,127	0,024
<i>Scenario 10</i>	0,019	-0,01	0,001
<i>Scenario 11</i>	0,004	-0,018	0,001
<i>Scenario 12</i>	0,181	-0,153	0,031
<i>Scenario 13</i>	0,066	-0,055	0,011
<i>Scenario 14</i>	0,044	-0,053	0,009
<i>Scenario 15</i>	0,137	-0,194	0,025
<i>Scenario 16</i>	0,179	-0,098	0,025
<i>Scenario 17</i>	0,519	-0,265	0,082
<i>Scenario 18</i>	0,081	-0,168	0,024
<i>Scenario 19</i>	0,124	-0,019	0,011

6.3 Case C:

For the sensitivity analysis for case C, three parameters were selected:

- Time shift of the weather data.
- The optical efficiency of the collector.
- The thermal efficiency of the collector.

Regarding the optical efficiency, it was multiplied by 0.9 (90 %) and 1.1 (110 %). For the thermal efficiency, the polynomial model was used to account for the heat loss, so the same factor was used to multiply each of the coefficients of the equation.

<i>Scenarios</i>	<i>Time shift</i>	<i>Col. Opt. efficiency</i>	<i>Col. Thermal efficiency</i>
<i>Scenario 0</i>	0	0.632	1
<i>Scenario 1</i>	1	0.632	1
<i>Scenario 2</i>	0.5	0.632	1
<i>Scenario 3</i>	-1	0.632	1
<i>Scenario 4</i>	-0.5	0.632	1
<i>Scenario 5</i>	0	0.632	1.1
<i>Scenario 6</i>	0	0.632	0.9
<i>Scenario 7</i>	0	0.5688	1
<i>Scenario 8</i>	0	0.5688	1.1
<i>Scenario 9</i>	0	0.5688	0.9
<i>Scenario 10</i>	0	0.6952	1
<i>Scenario 11</i>	0	0.6952	1.1
<i>Scenario 12</i>	0	0.6952	0.9

Case C

Control Volume	Energy to load	
	nRMSE	%DIF
<i>Parametric analysis</i>		
<i>Scenario 1</i>	0,1992	2,71
<i>Scenario 2</i>	0,1424	0,75
<i>Scenario 3</i>	0,2113	0,25
<i>Scenario 4</i>	0,1402	-0,40
<i>Scenario 5</i>	0,0459	0,15
<i>Scenario 6</i>	0,0511	-0,11
<i>Scenario 7</i>	0,1864	2,97
<i>Scenario 8</i>	0,1886	3,20
<i>Scenario 9</i>	0,1854	2,73
<i>Scenario 10</i>	0,1996	-2,13
<i>Scenario 11</i>	0,1963	-1,96
<i>Scenario 12</i>	0,2066	-2,22

Case C

Control Volume	Energy to load		
	Maximum normalized residual error	Minimum normalized residual error	Standard deviation
<i>Parametric analysis</i>			
<i>Scenario 1</i>	1,455	-1,447	0,139
<i>Scenario 2</i>	1,484	-1,421	0,1
<i>Scenario 3</i>	1,377	-1,474	0,149
<i>Scenario 4</i>	1,501	-1,474	0,099
<i>Scenario 5</i>	1,514	-0,227	0,032
<i>Scenario 6</i>	0,229	-1,474	0,036
<i>Scenario 7</i>	1,453	-0,255	0,129
<i>Scenario 8</i>	1,446	-0,257	0,131
<i>Scenario 9</i>	1,459	-0,254	0,129
<i>Scenario 10</i>	0,251	-1,474	0,14
<i>Scenario 11</i>	0,247	-1,474	0,18
<i>Scenario 12</i>	0,256	-1,474	0,144

6.4 Case D:

Scenarios	Time Shifting	HX Efectiveness (%)	Therm. Capac. Mult. Fac	Shading
Scenario 0	0	81	1	Partial
Scenario 1	1	81	1	Partial
Scenario 2	0.5	81	1	Partial
Scenario 3	-1	81	1	Partial
Scenario 4	-0.5	81	1	Partial
Scenario 5	0	60	1	Partial
Scenario 6	0	70	1	Partial
Scenario 7	0	90	1	Partial
Scenario 8	0	99	1	Partial
Scenario 9	0	81	0.6	Partial
Scenario 10	0	81	0.8	Partial
Scenario 11	0	81	1.2	Partial
Scenario 12	0	81	1.4	Partial
Scenario 13	0	81	1	No Shading
Scenario 14	0	81	1	On/Off

Case D Results

Control Volume	Energy to load	
	nRMSE	%DIF
Parametric analysis		
Scenario 1	0,877	-5,193
Scenario 2	0,529	-4,446
Scenario 3	0,873	-0,863
Scenario 4	0,475	-1,605
Scenario 5	0,028	-0,781
Scenario 6	0,013	-0,319
Scenario 7	0,005	0,103
Scenario 8	0,007	0,125
Scenario 9	0,068	1,264
Scenario 10	0,033	0,606
Scenario 11	0,032	-0,559
Scenario 12	0,061	-1,076
Scenario 13	0,626	13,257
Scenario 14	1,080	-21,619

Case D Results

Control Volume	Energy to load		
	Maximum normalized residual error	Minimum normalized residual error	Standard deviation
<i>Scenario 1</i>	1,114	-1,344	0,115
<i>Scenario 2</i>	0,598	-0,877	0,069
<i>Scenario 3</i>	1,308	-1,134	0,115
<i>Scenario 4</i>	0,705	-0,733	0,063
<i>Scenario 5</i>	0,03	-0,009	0,004
<i>Scenario 6</i>	0,019	-0,006	0,002
<i>Scenario 7</i>	0,004	-0,016	0,001
<i>Scenario 8</i>	0,006	-0,019	0,001
<i>Scenario 9</i>	0,007	-0,064	0,009
<i>Scenario 10</i>	0,003	-0,032	0,005
<i>Scenario 11</i>	0,032	-0,006	0,004
<i>Scenario 12</i>	0,064	-0,005	0,009
<i>Scenario 13</i>	0,007	-0,678	0,081
<i>Scenario 14</i>	1,484	-0,002	0,158

7 Conclusions and outlook

This work shows a summary of the results obtained by the comparison campaign of the simulation tools used to evaluate SHIP plants yields. Currently, there are a large number of public and private simulation tools available for the study and evaluation of solar technologies; however, there is a lack of standardized methodologies that collect the vast international experience of the scientific community. These standardized methodologies would reduce inadvertent errors that can significantly impact the performance and design of the schemes. In addition, it was noticed that most of the project developers use their in-house developed tools; however, certain tools have been developed to model specific systems and do not perform appropriately for technologies different from the original.

The analysis of simulation results of Cases A, B, C, and D obtained using different simulation tools and scenarios with induced errors studied shows significant differences in each control volume studied. The statistical results show that although there are simulation tools that can reproduce statistical distributions similar to the reference, the assumptions and models involved, which are highly nonlinear, propagate errors that can be compensated to a lesser extent by the applied control system and/or largely by the energy storage system. Despite the results above, the energy dispatched towards the energy demand shows overestimates or underestimates with differences that can reach 41% at an annual level (see Table 3 Case D, tool 2), while this same case shows the greatest error due to PTC field sensitivity to shading error. Furthermore, the complementarity between the analysis has made it possible to identify through the DTW that there are differences in terms of the dynamics of the time series, observing a wide range of values between the maximum and minimum limits found. Within Subtask C, the results obtained by each simulation tool and the normalized errors can be used as a reference to demonstrate the impact of each induced error and the simulation differences between simulation tools, but also the limitations of the assumptions to obtain acceptable results with errors less than 10%.


8 References

- Brown, M., and L. Rabiner. 2005. "Dynamic Time Warping for Isolated Word Recognition Based on Ordered Graph Searching Techniques." In *ICASSP '82. IEEE International Conference on Acoustics, Speech, and Signal Processing*. Institute of Electrical and Electronics Engineers. <https://doi.org/10.1109/icassp.1982.1171695>.
- Cardemil, José M., Ignacio Calderón-Vásquez, Alan Pino, Allan Starke, Ian Wolde, Carlos Felbol, Leonardo F. L. Lemos, et al. 2022. "Assessing the Uncertainties of Simulation Approaches for Solar Thermal Systems Coupled to Industrial Processes." *Energies* 15 (9): 1–29.
- Farjana, Shahjadi Hisan, Nazmul Huda, M. A. Parvez Mahmud, and R. Saidur. 2018. "Solar Process Heat in Industrial Systems – A Global Review." *Renewable and Sustainable Energy Reviews* 82 (February): 2270–86.
- Gaspar, Martin, Bastian Welke, Frank Seehaus, Christof Hurschler, and Michael Schwarze. 2017. "Dynamic Time Warping Compared to Established Methods for Validation of Musculoskeletal Models." *Journal of Biomechanics* 55 (April): 156–61.
- Li, Huanhuan, Jingxian Liu, Zaili Yang, Ryan Wen Liu, Kefeng Wu, and Yuan Wan. 2020. "Adaptively Constrained Dynamic Time Warping for Time Series Classification and Clustering." *Information Sciences* 534 (September): 97–116.
- Quiñones, Gonzalo, Carlos Felbol, Carlos Valenzuela, Jose M. Cardemil, and Rodrigo A. Escobar. 2020. "Analyzing the Potential for Solar Thermal Energy Utilization in the Chilean Copper Mining Industry." *Solar Energy* 197 (February): 292–310.
- Santos López, Guillermo de. 2021. "Techno-Economic Analysis and Market Potential Study of Solar Heat in Industrial Processes." Edited by Rafael Guedez. Master of Science, KTH Royal Institute of Technology.
- Sharma, Ashish K., Chandan Sharma, Subhash C. Mullick, and Tara C. Kandpal. 2017. "Solar Industrial Process Heating: A Review." *Renewable and Sustainable Energy Reviews* 78 (October): 124–37.
- Weiss, Werner, and Monika Spörk-Dür. (2020) 2020. "Solar-Heat-Worldwide 2020." IEA - Solar Heating and Cooling Programme.
- Zhang, James, Michael Johnstone, Vu Le, Burhan Khan, Mohammad Anwar Hosen, Doug Creighton, Jessica Carney, Andy Wilson, and Michael Lynch. 2021. "Dynamic Time Warp-Based Clustering: Application of Machine Learning Algorithms to Simulation Input Modelling." *Expert Systems with Applications* 186 (December): 115684.

9 Appendix: Simulation Tools for Solar Thermal Systems

Software Name	State	Scope	Design Flexibility	Economical Prefeasibility Analysis	Licensing	Developing institution	Homepage
CEA (SHIP2FAIR)	Operational	Research/ Professional Design	User Defined Schemes	Yes	Under Development	CEA, in the context of the SHIP2FAIR European Project	http://ship2fair-h2020.eu/
GREENIUS	Operational	Simple Design	Predefined Schemes	Yes	Freeware	DLR, German Aerospace Center	http://freegreenius.dlr.de
NEWHeat - OWN	Operational	Research/ Professional Design	User Defined Schemes	Yes		NEWHeat. It was developed to perform their own simulations and verifications	
POLYSUN	Operational	Research/ Professional Design	User Defined Schemes	Yes	Commercial	Vela Solaris	http://www.velasolaris.ch
System Advisor Model (SAM)	Operational	Research	Predefined Schemes	Yes	Open Source	NREL, National Renewable Energy Laboratory, USA	Home - System Advisor Model (SAM) (nrel.gov)
Transient System Simulation Tool (TRNSYS)	Operational	Research	User Defined Schemes	Yes	Commercial	Univ. Wisconsin, Solar Energy, Lab. Madison, USA	http://sel.me.wisc.edu/trnsys/
COLSIM	Operational	Research		Yes	Free online	Fraunhofer ISE	https://www.colsim.org/
COLSIM CSP	Operational	Research	User Defined Schemes	Yes	Internal Use	Fraunhofer ISE	
Prosol simulation tool	No Operational	-				Politecnico Milano	-
SOLTERM	Operational	Simple Design	Predefined Schemes	Yes	Commercial	LNEG, IP (Portugal)	solterm5 LNEG Laboratório Nacional de Energia e Geologia

Software Name	State	Scope	Design Flexibility	Economical Prefeasibility Analysis	Licensing	Developing institution	Homepage
T*SOL Pro	Operational	Professional design	User Defined Schemes	Yes	Commercial	Dr. Valentin Energie Software GmbH	T*SOL – Valentin Software GmbH (valentin-software.com)
SOPRO	No Operational	Simple Design	Predefined Schemes	No	Internal Use	Fraunhofer ISE	Offline
Appsol-Therm	Operational		Predefined Schemes	Yes	Free online	Appsol	Appsol – Energía solar para industria
Engineering Equation Solver (EES)	Operational	Simple Design/ Research	-	No	Commercial	F- Chart Software	EES: Engineering Equation Solver F-Chart Software : Engineering Software
Environmental Life-cycle Impacts of Solar Airconditioning systems (ELISA)	Operational	Research	Predefined Schemes	No	Freeware	Universidad de Palermo	IEA SHC Task 53 Software/Tools (iea-shc.org)
F-Chart	Operational	Simple Design	Predefined Schemes	Yes	Commercial	SA Klein & WA Beckman - F-Chart Software	F-CHART: Solar Systems Analysis F-Chart Software : Engineering Software
HOMER	Operational	Professional Design	Predefined Schemes	Yes	Commercial	UL - NREL	HOMER - Hybrid Renewable and Distributed Generation System Design Software (homerenergy.com)
IKI Solar Payback Calculator	Operational	Simple Design	Predefined Schemes	Yes	Freeware	Fraunhofer ISE	Solar Heat for Industry Economic Potential (solar-payback.com)
Insel	Operational	Research/ Professional Design	User Defined Schemes	Yes	Commercial	INSEL.eu	INSEL - Homepage - INSEL en

Software Name	State	Scope	Design Flexibility	Economical Prefeasibility Analysis	Licensing	Developing institution	Homepage
optiCAD	No Operational	Optical simulation		No	Commercial	OptiCAD Corporation	(OFFLINE) www.opticad.com
Ressspi	Operational	Research/ Professional Design	Predefined Schemes	Yes	Free online	SOLATOM	Ressspi , the solar simulator for industrial processes
RETScreen Expert	Operational	Simple Design	Predefined Schemes	Yes	Commercial	CanmetENERGY	RETScreen (nrcan.gc.ca)
SHIPCal-CIMAV	Operational	Simple Design/ Research	Predefined Schemes	Yes	Free online	Centro de Investigación en Materiales Avanzados.	http://shipcal.cimav.edu.mx/accounts/login/
SHIP CALCULATOR	Operational	Research	Predefined Schemes	Yes	Freeware	Fraunhofer Institute for Solar Energy Systems.	File:20190301 SHIP Feasibility Calculator.xlsx — energypedia.info
SHIP Desing Tool	No Operational	Research		No	Free online	Hochschule fur Technik Stuttgart	(OFFLINE) https://www.fp7-insun.eu/
Solar Plant Sizing and Layout	Operational	Professional Design	User Defined Schemes	Yes	Free online	SOLARE PROZESSWARME	Solar Plant Sizing and Layout — Solare Prozesswärme (xn—solare-prozesswrme-ztb.info)
Transol	No Operational	Professional Design	Predefined Schemes	Yes	Commercial	AIGUASOL & Centre Scientifique et Technique du Bâtiment	Software para el diseño, optimización y gestión energética de sistemas solares térmicos, TRANSOL – Aiguasol
T53E4	Operational	Simple Design	Predefined Schemes	Yes	Free online	Universität Innsbruck & DanielNeyer Brainworks.	IEA SHC Task 53 Software/Tools (iea-shc.org)
Thermal Engineering Systems in Python (TESpy)	Operational	Simple Design/ Research	User Defined Schemes	No	Open Source		Libraries (oemof.org)

